The Effect of $CH_3NH_3PbI_3$ Concentration Precursor on the $TiO_2/CH_3NH_3PbI_3$ Thin Film Morphology in Perovskite Solar Cell

Noor Fadhilah Ramli, Suhaila Sepeai, Nur Fairuz Mohd Rostan, Norasikin Ahmad Ludin, Mohd. Adib Ibrahim, Mohd Asri Mat Teridi and Saleem H.Zaidi
Solar Energy Research Institute (SERI)
University Kebangsaan Malaysia (UKM)
Selangor, Malaysia
fadhilah0129@gmail.com, suhailas@ukm.edu.my, fairuzmydr@gmail.com, sheekeen@ukm.edu.my, mdadib@ukm.edu.my, asri@ukm.edu.my, saleemzaidi@ukm.edu.my

***Abstract*—Surface morphology and film formation of every functional layer are crucial parameters of the perovskite solar cell. However, imprecise control of concentration, solvent choice, composition and annealing temperature affect the crystallization process cause unwanted defects such as pinholes and grain boundaries. In this study, the thin film of titanium oxide/methylammonium lead iodide ($TiO_2/CH_3NH_3PbI_3$) was deposited on fluorine-doped tin oxide (FTO) glass by one-step solution technique and the concentrations of $CH_3NH_3PbI_3$ were controlled to optimize surface morphology and film formation. The smooth and uniform of $CH_3NH_3PbI_3$ thin film formation with a low amount of voids and high absorbance were yielded regarding the increased concentration of $CH_3NH_3PbI_3$ precursor solution. Additionally, the chlorobenzene (CBZ) dripping enhanced the uniformity $CH_3NH_3PbI_3$ thin film. A good correlation between the surface morphology of $TiO_2/CH_3NH_3PbI_3$ thin film and UV-Vis absorbance spectra were also obtained in this study.**

Keywords—concentration; methylammonium lead iodide; surface morphology; absorbance spectra

I. Introduction

Perovskite solar cells (PSCs) gained a great attention in solar cell research due to its fast-growing performance of efficiency up to 22.1 % within approximately ten years [1]. A key success of the PSCs is mostly attributed to strong absorbing direct bandgap with ~1.6 eV, high carrier mobilities [2], shallow defect levels [3] and the long diffusion length of charge carriers in the absorber perovskite layer [4]. These parameters are expected to depend strongly on film crystallinity and morphology.

Perovskites exhibit the simple AMX_3 (cations, A, metal, M, anion, X,) base configuration that rich in diversity of composition, structure, and properties [5]. The great interest of the organometal halide CH_3NH_3 MX_3 (M = Pb or Sn, X = Cl, Br or I) due to its efficient light harvesting. This perovskite material is stabilized mostly as a tetragonal crystal structure at an ambient temperature and is compatible with both solution processing and evaporation techniques [6]. Moreover, the $CH_3NH_3PbI_3$ thin film was simply prepared from methylammonium iodide (MAI) and lead (II) iodide PbI_2 precursors through a simple one-step solution process, which is inexpensive fabrication and ease of processing [7]–[9].

The best fabrication technique of the PSCs also becomes one of the important factors to attain the success of the development this type of solar cell. In recent years, the solution-processing becomes the best and common fabrication technique for thin-film solar cells especially PSCs. The solution-processing includes spin-coating, blade-coating, spraying, inkjet printing, gravure printing, or slot-dye coating [8]. However, lacking skill implementation during these processes especially one-step solution process (spin-coating) can affect the performances of perovskite solar cell. Therefore, some parameters must be taken into account such as solution concentration, solvent choice, composition, annealing temperature etc.

As the film crystallinity and morphology are significant parameters to develop high-performance PSCs, thus morphology quality of the perovskite thin films must precisely control. However, it is not easy to precisely control the thickness, uniformity and composition of precursor to improve the crystallinity and morphology of the PSCs. Therefore, this study puts some efforts to improve and enhance the film morphology of $CH_3NH_3PbI_3$ as it is widely used and has a reliable absorber property. As one-step solution process is simple and eases in processing, the process will be used by controlling the concentration of $CH_3NH_3PbI_3$ precursor solution. The chlorobenzene was used as anti-solvent to improve the crystallinity and morphology. The implementation of anti-solvent is proven effectively assist the perovskite crystallization process [10].

Therefore, this study emphasized the film morphology such as surface roughness regarding the concentration of $CH_3NH_3PbI_3$ precursor solution by atomic force microscopy (AFM) scan. In addition, the optical property such as UV-Vis absorbance spectra and the correlation between this film morphology and optical property of $CH_3NH_3PbI_3$ precursor solution were also been discussed.

This work supported Universiti Kebangsaan Malaysia under Geran Universiti Penyelidikan project (GUP-2017-077).

II. EXPERIMENTAL SECTION

A. Substrate and $CH_3NH_3PbI_3$ Precursor Preparation

The 2x2 cm^2 FTO glasses (Solaronix, 15 Ω/sq) were cleaned and sonicated with acetone, ethanol and isopropanol in an ultrasonic bath, each for 15 minutes. Then, the nitrogen gas was used to purge the glasses. A compact TiO_2 layer was formed through the spin-coating of TiO_2 blocking layer solution at 3000 rpm for 35 s and subsequently annealed at 500 °C for 60 minutes. A TiO_2 blocking layer (Dyesol, Bl-1) was diluted by ethanol with a ratio of 1:9 to prepare the TiO_2 blocking layer solution.

To form the $CH_3NH_3PbI_3$ precursor solution, methylammonium iodide (MAI) and lead (II) iodide (PbI_2) (Sigma-Aldrich) were dissolved in anhydrous N, N-Dimethylformamide (DMF), at a 1:1 molar ratio of MAI to PbI_2. To explore the effect of the concentration of $CH_3NH_3PbI_3$ precursor solution on the $TiO_2/CH_3NH_3PbI_3$ films, four types of $CH_3NH_3PbI_3$ precursor solutions with different concentrations (0.8 M, 1.0 M, 1.2 M, and 1.4 M) were prepared.

B. $TiO_2/CH_3NH_3PbI_3$ Thin Film Fabrication and Thin Film Characterization

To form the perovskite layer, the $CH_3NH_3PbI_3$ precursor was spin-coated on the substrate with TiO_2 blocking layer in a nitrogen filled glovebox, at 3000 rpm for 25 seconds. 5 seconds before the end of the last spin coating step, chlorobenzene (CBZ) was dripped onto the rotating sample, which resulted in an improved uniformity of the $CH_3NH_3PbI_3$ crystal growth. The sample was then annealed at 100°C for 60 minutes.

The absorption was characterized by LAMBDA 950/1050 UV/VIS/NIR Spectrophotometer from Perkin Elmer. The surface morphology images were obtained from atomic force microscopy (AFM). The thickness of the $TiO_2/CH_3NH_3PbI_3$ thin film was measured by a DEKTAK 150 Surface Profiler from Veeco.

III. RESULTS AND DISCUSSION

MAI and PbI_2 dissolved in the DMF solvent by ratio 1:1 was employed as the precursor solution. The concentration of precursor solutions was varied into four types; 0.8 M, 1.0 M, 1.2 M and 1.4 M respectively. In this study, the one-step deposition technique is used where the $CH_3NH_3PbI_3$ precursor solution was spin-coated on the FTO glass and followed by dripping CBZ as antisolvent. The detailed preparation process of $TiO_2/CH_3NH_3PbI_3$ films as described as following; the perovskite precursor solution is deposited onto the compact TiO_2 coated substrate by spin coating at 3000 rpm for 25 seconds and the antisolvent was dropped at last 5 seconds. The deposited film was annealed at 100 °C for 60 minutes on the hot plate.

From the observation, the formation process of $CH_3NH_3PbI_3$ films can be divided into two stages. The first stage is the nucleation of the intermediate of MAI: PbI_2 during the spin coating induced by solvent evaporation, while the second stage is the structural transformation from the intermediate of CBZ. CBZ plays the important role in the formation of the $CH_3NH_3PbI_3$ film due to its behaviour delays the transformation structure and crystal growth of $CH_3NH_3PbI_3$ until annealing process [11]. Hence, the result showed that the $CH_3NH_3PbI_3$ films are smoothly formed onto FTO glass with TiO_2 layer and the colour of $CH_3NH_3PbI_3$ precursor solution was changed into dark brown right after the spin coating process. Without the dripping of CBZ, the reaction of lead iodide (PbI_2) and methylammonium iodide (MAI) is quite fast during spin-coating and the effect of fast crystallization of this perovskite material. The $CH_3NH_3PbI_3$ film formation without CBZ can be seen in Fig. 1 (a). Fig. 1 (b) shows the diagram of the formation of the TiO2/CH3NH3PbI3 film on the FTO glass with dripping CBZ at last 10 seconds and it does not show a good film formation. This is due to the liquid film starts to dry after 7 seconds and the addition of CBZ does not improve the film formation [11]. Fig. 1 (c) shows a quite good $CH_3NH_3PbI_3$ film formation by dripping CBZ at last 5 seconds and has a good agreement with the previous study [11].

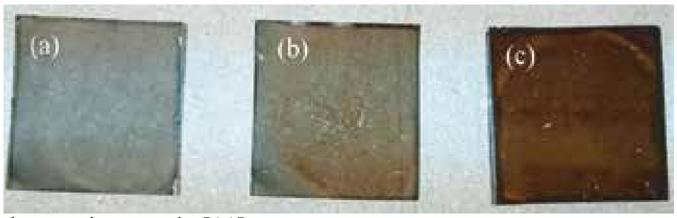

Fig. 1. (a) $TiO_2/CH_3NH_3PbI_3$ films formation on the FTO glass without chlorobenzene, (b) with chlorobenzene dripping at last 10 seconds and (c) with chlorobenzene dripping at last 5 seconds.

A. TiO_2/ $CH_3NH_3PbI_3$ Film Morphology

As the concentration of $CH_3NH_3PbI_3$ precursor solution was varied into four types of concentration; 0.8 M, 1.0 M, 1.2 M and 1.4 M, there are some morphology effects that can be indicated through Surface Profiler and AFM scans. The thickness of the perovskite films that was measured by Surface Profiler was in the range of 520 nm to 1200 nm by increased the concentration of $CH_3NH_3PbI_3$ precursor solution from 0.8 M to 1.4 M. Thus, it can be indicated that the thickness of the perovskite layer is increased with the increasing of precursor concentration.

Fig. 2 shows the topography and 3D images of 0.8 M, 1.0 M, 1.2 M and 1.4 M of $CH_3NH_3PbI_3$ precursor solution that obtained from AFM scans. The scanning area for the measurement was 3×3 μm^2 and randomly chosen from a large and uniform perovskite film with a size of 2 cm^2. The topography images indicated that the surface structure of the $CH_3NH_3PbI_3$ film formation corresponding to the concentration. It can be seen in Fig. 2 (c) and (d) that the surface structures of the 1.2 M and 1.4 M $CH_3NH_3PbI_3$ were smoother than 0.8 M and 1.0 M $CH_3NH_3PbI_3$ with similar grain sizes. However, there was some large size of grains on the surface structures of 0.8 M and 1.0 M $CH_3NH_3PbI_3$. The corresponding root-mean-square (RMS) roughness values of 22.13, 19.62, 11.76 and 9.32 nm were obtained for films prepared by 0.8 M, 1.0 M, 1.2 M and 1.4 M of perovskite precursor solution respectively. From the 3D images of 0.8 M and 1.0 M $CH_3NH_3PbI_3$, the surfaces were unsmooth by high

RMS value because of there were some uneven grains can be seen be on the surface in Fig. 2 (a) and (b). The rough surface is a drawback to the device performance due to its high probability of penetrating through the hole transport material [12] and caused light depolarization [13] that affect the efficiency of perovskite solar cell.

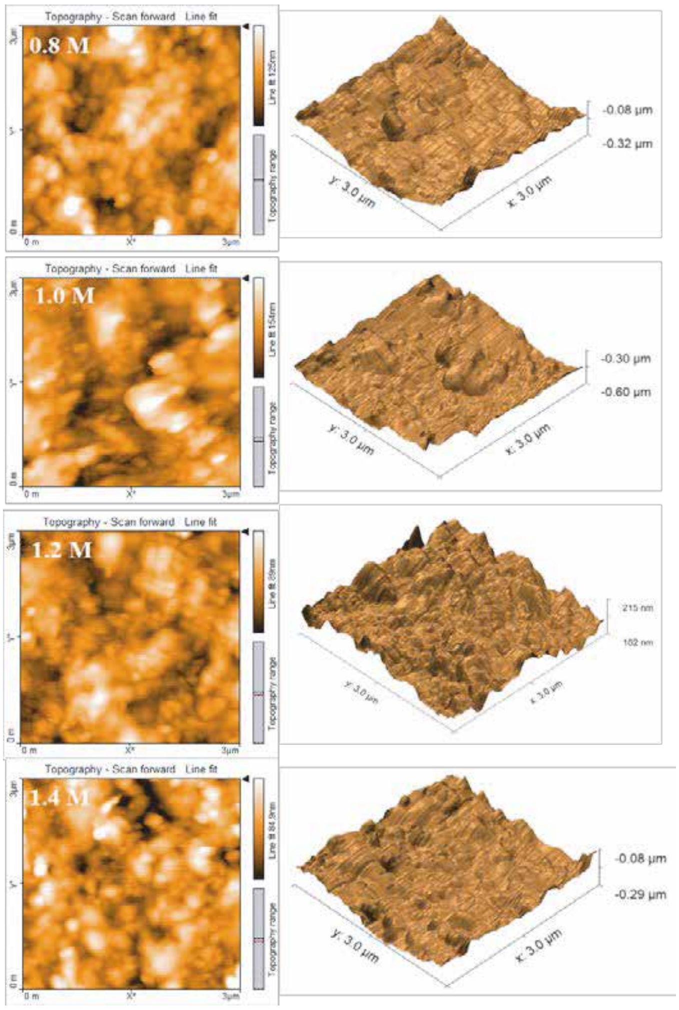

Fig. 2. The topography and 3D images of 0.8 M, 1.0 M, 1.2 M and 1.4 M of $CH_3NH_3PbI_3$ precursor solution.

Based on the previous studies, some improvement of crystal growth and surface morphology had successfully obtained by either controlling CH_3NH_3I or PbI_2 concentration to enhance the performances of perovskite solar cell [14]–[16]. This study gave some efforts to the one-step solution technique by controlling the $CH_3NH_3PbI_3$ concentration and it indicated the good results on the surface morphology especially on the surface roughness.

B. Optical Properties of $TiO_2/CH_3NH_3PbI_3$ Film

UV-Vis absorbance spectra obtained in Fig. 3 were directly proportional to 0.8 M, 1.0 M, 1.2 M and 1.4 M $CH_3NH_3PbI_3$ concentrations were in a good agreement with the previous report [17]. The range of absorption wavelength for these films was from 750 nm to 800 nm, and the maximum absorption wavelength was consistent with the bandgap value of $CH_3NH_3PbI_3$, which is approximately 1.6 eV. The 0.8 M $CH_3NH_3PbI_3$ film obtained the lowest absorbance spectra, due to its low surface roughness. The modification of concentration 1.0 M, 1.2 M and 1.4 M $CH_3NH_3PbI_3$ was the reason for higher absorbance because of a better surface morphology of perovskite films in term of surface roughness and crystalline growth. This had shown the significant correlation between the absorbance and the surface morphology of perovskite film. The film surface for 1.4 M $CH_3NH_3PbI_3$ was darker in brown colour than the other films with different concentrations that shown in the Fig. 4. Besides, some voids can be clearly seen in the large-scale area (2 cm^2) of 1.4 M $CH_3NH_3PbI_3$ surface film. Therefore, the UV-Vis absorbance spectra of these different concentrations did not only depend on the surface morphology of $CH_3NH_3PbI_3$ film but also proved the Beer-Lambert's Law.

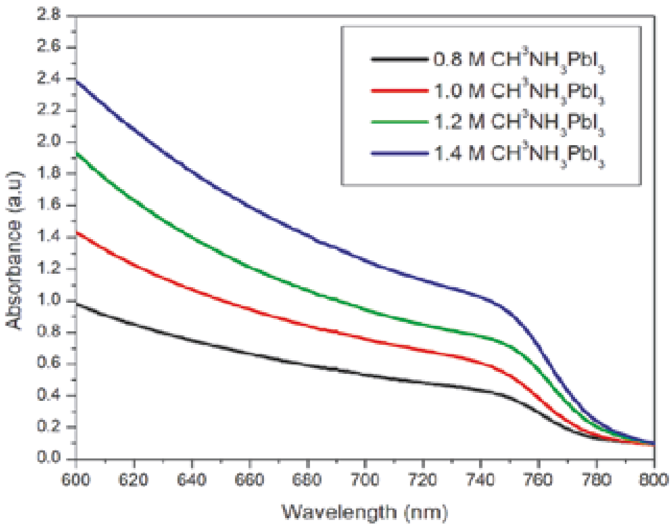

Fig. 3. UV-Vis absorbance spectra of 0.8 M, 1.0 M, 1.2 M and 1.4 M $CH_3NH_3PbI_3$ films.

Based on the Beer-Lambert's Law, the absorbance is linearly proportional to the concentration of absorbing species that is corresponding to the attenuation of light when the light is travelling through the properties of the material. This UV-Vis data were coinciding to the Beer-Lambert's Law as expected which the increase of concentration $CH_3NH_3PbI_3$ precursor solution had affected the attenuation of light travelling. This is due to the light was absorbed by the thickness of the $CH_3NH_3PbI_3$ films. As stated in the previous section, the thicknesses of the $CH_3NH_3PbI_3$ film were related to the concentration. Thus, the absorbance was increased accordingly to the increased of $CH_3NH_3PbI_3$ precursor solution concentration.

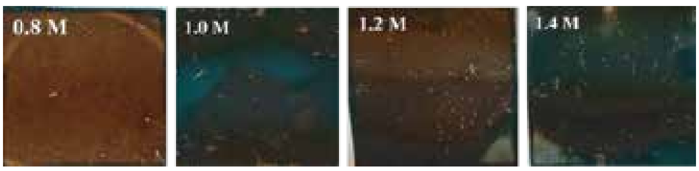

Fig. 4. The $TiO_2/CH_3NH_3PbI_3$ films on FTO glass with 0.8 M, 1.0 M, 1.2 M and 1.4 M $CH_3NH_3PbI_3$ precursor concentrations.

IV. CONCLUSION

In conclusion, this study had developed $TiO_2/CH_3NH_3PbI_3$ films with different concentrations of $CH_3NH_3PbI_3$ precursor solution, namely 0.8 M, 1.0 M, 1.2 M and 1.4 M. One-step solution deposition was used and yielded a good surface performance to the $TiO_2/CH_3NH_3PbI_3$ films. The smooth and low surface roughness films were produced regarding the increase in the concentration of $CH_3NH_3PbI_3$ precursor solution and precise dripping technique of CBZ. A good correlation between surface roughness (surface morphology) and concentration $CH_3NH_3PbI_3$ precursor solution was obtained. The high absorbance was yielded from the increased of concentration $CH_3NH_3PbI_3$ precursor solution as expected.

ACKNOWLEDGEMENT

The authors would like to thank Solar Energy Research Institute (SERI) staff and Mohammad Firdaus Mohd Noh for the kind help in running the equipment for characterizations. This work has been carried out with the support of Universiti Kebangsaan Malaysia under Geran Universiti Penyelidikan project (GUP-2017-077).

REFERENCES

[1] D. Zhao, Y. Yu, C. Wang, W. Liao, N. Shrestha, C. R. Grice, A. J. Cimaroli, L. Guan, R. J. Ellingson, K. Zhu, X. Zhao, R.-G. Xiong, and Y. Yan, "Low-Bandgap Mixed Tin–Lead Iodide Perovskite Absorbers with Long Carrier Lifetimes for All-Perovskite Tandem Solar Cells," *Nat. Energy*, vol. 2, no. 4, p. 17018, 2017.

[2] J. W. Xiao, L. Liu, D. Zhang, N. De Marco, J. W. Lee, O. Lin, Q. Chen, and Y. Yang, "The Emergence of the Mixed Perovskites and Their Applications as Solar Cells," *Adv. Energy Mater.*, vol. 7, no. 20, p. 1700491, 2017.

[3] W.-J. Yin, J.-H. Yang, J. Kang, Y. Yang, and S.-H. Wei, "Halide Perovskite Materials for Solar Cells: A Theoretical Review," *J. Mater. Chem. A*, vol. 3, no. 17, pp. 8926–8942, 2015.

[4] D. Shi, V. Adinolfi, R. Comin, M. Yuan, E. Alarousu, A. Buin, Y. Chen, S. Hoogland, A. Rothenberger, K. Katsiev, Y. Losovyj, X. Zhang, P. A. Dowben, O. F. Mohammed, E. H. Sargent, and O. M. Bakr, "Low Trap-State Density and Long Carrier Diffusion in Organolead Trihalide Perovskite Single Crystals," *Science (80-.).*, vol. 347, no. 6221, p. 519, 2015.

[5] P. P. Boix, S. Agarwala, T. M. Koh, N. Mathews, and S. G. Mhaisalkar, "Perovskite Solar Cells: Beyond Methylammonium Lead Iodide," *J. Phys. Chem. Lett.*, vol. 6, no. 5, pp. 898–907, 2015.

[6] H. S. Jung and N. G. Park, "Perovskite solar cells: From Materials to Devices," *Small*, vol. 11, no. 1, pp. 10–25, 2015.

[7] M. I. Ahmed, A. Habib, and S. S. Javaid, "Perovskite Solar Cells: Potentials, Challenges, and Opportunities," *Int. J. Photoenergy*, vol. 2015, pp. 1–13, 2015.

[8] G. E. Eperon, V. M. Burlakov, P. Docampo, A. Goriely, and H. J. Snaith, "Morphological Control for High Performance, Solution-Processed Planar Heterojunction Perovskite Solar Cells," *Adv. Funct. Mater.*, vol. 24, no. 1, pp. 151–157, 2014.

[9] Z. Song, S. C. Watthage, A. B. Phillips, and M. J. Heben, "Pathways Toward High-Performance Perovskite Solar Cells: Review of Recent Advances in Organo-Metal Halide Perovskites for Photovoltaic Applications," *J. Photonics Energy*, vol. 6, no. 2, p. 22001, 2016.

[10] K. A. Bush, A. F. Palmstrom, Z. J. Yu, M. Boccard, R. Cheacharoen, J. P. Mailoa, D. P. Mcmeekin, R. L. Z. Hoye, C. D. Bailie, T. Leijtens, I. M. Peters, M. C. Minichetti, N. Rolston, R. Prasanna, S. Sofia, D. Harwood, W. Ma, F. Moghadam, H. J. Snaith, T. Buonassisi, Z. C. Holman, S. F. Bent, and M. D. Mcgehee, "23.6%-Efficient Monolithic Perovskite/Silicon Tandem Solar Cells with Improved Stability," *Nat. Energy*, vol. 2, no. 4, p. 17009, 2017.

[11] M. Konstantakou, D. Perganti, P. Falaras, and T. Stergiopoulos, "Anti-Solvent Crystallization Strategies for Highly Efficient Perovskite Solar Cells," *Crystals*, vol. 7, no. 10, p. 291, 2017.

[12] Y. Yu, S. Yang, L. Lei, Q. Cao, J. Shao, S. Zhang, and Y. Liu, "Ultrasmooth Perovskite Film via Mixed Anti-Solvent Strategy with Improved Efficiency," *ACS Appl. Mater. Interfaces*, vol. 9, no. 4, pp. 3667–3676, 2017.

[13] P. Löper, M. Stuckelberger, B. Niesen, J. Werner, M. Filipič, S.-J. Moon, J.-H. Yum, M. Topič, S. De Wolf, and C. Ballif, "Complex Refractive Index Spectra of CH3NH3PbI3 Perovskite Thin Films Determined by Spectroscopic Ellipsometry and Spectrophotometry," *J. Phys. Chem. Lett*, vol. 6, no. 1, pp. 66–71, 2014.

[14] J.-H. Im, I.-H. Jang, N. Pellet, M. Grätzel, and N.-G. Park, "Growth of CH3NH3PbI3 Cuboids with Controlled Size for High-Efficiency Perovskite Solar Cells," *Nat. Nanotechnol.*, vol. 9, no. 11, pp. 927–932, 2014.

[15] D. Bi, J. Luo, F. Zhang, A. Magrez, E. N. Athanasopoulou, A. Hagfeldt, and M. Grätzel, "Morphology Engineering: A Route to Highly Reproducible and High Efficiency Perovskite Solar Cells," *ChemSusChem*, vol. 10, no. 7, pp. 1624–1630, 2017.

[16] N.-G. Park, "Methodologies for High Efficiency Perovskite Solar Cells," *Nano Converg.*, vol. 3, no. 1, p. 15, 2016.

[17] K. Fu, S. S. Lim, Y. Fang, P. P. Boix, N. Mathews, T. C. Sum, L. H. Wong, and S. Mhaisalkar, "Modulating CH3NH3PbI3 Perovskite Crystallization Behavior Through Precursor Concentration," *Nano*, vol. 9, no. 5, p. 1440003, 2014.